NASA TECHNICAL NOTE

NASA TN D-2958

NASA TN D-2958

AMPTIAC

61248

DISTRIBUTION STATEMENT A
Approved for Public Release
Distribution Unlimited

SIGNIFICANCE OF PHOTOGRAPHIC METEOR DATA IN THE DESIGN OF METEOROID PROTECTION FOR LARGE SPACE VEHICLES

Reproduced From
Best Available Copy

by Nestor Clough and Seymour Lieblein

Lewis Research Center
Cleveland, Ohio

20011210 157

NATIONAL AERONAUTICS AND SPACE ADMINISTRATION • WASHINGTON, D. C. • AUGUST 1965

NASA TN D-2958

SIGNIFICANCE OF PHOTOGRAPHIC METEOR DATA IN THE DESIGN OF METEOROID PROTECTION FOR LARGE SPACE VEHICLES

By Nestor Clough and Seymour Lieblein

Lewis Research Center
Cleveland, Ohio

NATIONAL AERONAUTICS AND SPACE ADMINISTRATION

For sale by the Clearinghouse for Federal Scientific and Technical Information
Springfield, Virginia 22151 – Price $2.00

SIGNIFICANCE OF PHOTOGRAPHIC METEOR DATA IN THE DESIGN OF METEOROID PROTECTION FOR LARGE SPACE VEHICLES

by Nestor Clough and Seymour Lieblein

Lewis Research Center

SUMMARY

Described herein are the method of obtaining photographic meteor data in the mass range of 10^{-2} to 10^{0} gram and the treatment of these data to provide useful engineering relations for protecting large space vehicle components against meteoroid impact. The assumptions needed to convert these data to meteoroid masses and densities are discussed, and the effects of these assumptions on design relations are shown. The inferred nature and values of meteoroid density, mass, and velocity are described, and an internally consistent meteoroid mass flux model is introduced for the photographic meteoroid range. Earth shielding factors as a function of satellite altitude are presented for use with the proposed model. Values of average meteoroid density and average meteoroid velocity relative to the Earth at the Earth's atmosphere lower than values previously used are indicated by an analysis of the available photographic meteor data. Photographic meteor astronomy is shown to be a significant source of data in describing the meteoroid hazard in space.

INTRODUCTION

The space vehicles and power generation systems of the future can be expected to have stringent requirements of long duration, large surface areas, and high probability of success placed upon them. Components of these flight systems, especially those containing fluid circuits and life support areas, will have to be protected against critical damage due to meteoroid impact. Components with especially large exposed surface areas are the propellant tanks of large chemical and nuclear rockets and the waste-heat radiators of power generation and coolant systems.

The critical meteoroid mass, or the mass of the largest meteoroid that the vehicle component must be protected against, increases with the vulnerable area, the exposure

time, and the probability of survival without critical damage (e.g., ref. 1). This relation indicates that large space system components must be protected against meteoroid particles with masses of the order of 10^{-2} to 10^{-4} gram. Of particular interest to the designer of such systems are meteoroid influx rate, density, structure, impact velocity, and direction of flight in this particular mass range. Since the design engineer cannot predict the exact conditions of these variables, he must rely on the probability of meeting specified conditions.

Numerous satellites and rockets have been launched in an attempt to count directly the particle flux in the near-Earth environment (e.g., ref. 2). The recent experiment, Explorer XVI, was the first satellite to measure directly perforation rates in pressurized cells. The energy-sensitive detectors of Explorer XVI recorded particle flux rates two to three orders of magnitude lower than the rates obtained by previously flown momentum-sensitive experiments for the 10^{-8} to 10^{-9} gram range (ref. 3). Preliminary reduction of these data in terms of a geocentric and a heliocentric distribution of near-Earth particles indicates a possible reduction in the apparent discrepancy.

Unfortunately, satellite measurements in the 10^{-8} to 10^{-9} gram range are from four to seven orders of magnitude from the range of interest for large space vehicle components, and the data cannot justifiably be extrapolated into this region. An experiment of the Explorer XVI type would be highly desirable in the 10^{-2} to 10^{-4} gram range. According to the best currently available estimates of the flux, however, a satellite with approximately 10^{5} square feet of vulnerable area and an exposure time of approximately 1 year would yield only one impact of a 10^{-2} gram particle. Directly applicable satellite experiments thus appear to be highly improbable at the moment.

The design engineer must therefore rely on indirect meteoroid data obtained by astronomical means (photographic, visual, and radar), which measure particles with masses 10^{-4} gram and larger. These meteor data fall well within the range of interest for the large long-duration space vehicles, and no unjustifiable extrapolation is necessary. Meteor astronomy is the general term defining the study of meteors. Specifically, a meteor is the streak of light caused by a meteoroid traveling at high velocity through the Earth's atmosphere. The study of meteor astronomy is therefore specifically limited (by definition) to these large particles that leave visible evidence of their passage. General usage of the term, however, has led to the incorporation of all particles (micrometeoroids to bolides) under this general heading; however, the discussion herein will be limited to photographic-size meteoroids (10^{-2} g and larger).

Considerable meteor data are available in the literature, and various estimates of influx rates, densities, and velocities based on these data have been proposed (e.g., refs. 4 to 6). Radical differences in influx rates and densities of meteoroids from proposal to proposal lead one to be concerned with the significance and accuracy of astronomically derived predictions. Order of magnitude differences appear in these various

proposals, and the design engineer is at a loss to understand the reason for such differences and the shortcoming of proposing average density, velocity, and influx rate as universally applicable. Use of these various proposals for space vehicle design criteria results in large differences in protection requirements and weight among design studies. It is important, then, to understand the capabilities and limitations of astronomical reduction procedures and how to interpret the data presented in terms of the particle characteristics and flux.

One of the objectives of this report is to explain how photographic meteor data have been transformed into meteoroid densities and influx rates through the laws of meteor physics. The assumptions necessary in the reduction of the data are discussed, and the confidence that can be placed on calculated protection requirements is shown. In addition, application of the reduced data is discussed and a consistent meteoroid model in the photographic region is presented.

METEOR PHYSICS

Description

Meteoritic particles are collectively referred to as meteoroids. Present knowledge of meteoroids suggests that they be classified into two major groups, with their origins designated as either cometary or asteroidal. The majority of meteoroids (in excess of 90 percent) are considered to be of cometary origin. These particles represent the debris left in space after cometary passage. The mechanism of injection and the type of particle injected are discussed in a following section. At this point, however, it is well to define terms associated with cometary meteoroids. A meteoroid shower is a periodic increase of meteoroid flux and represents a group of particles traveling in a definite, predictable orbit around the Sun. The fact that many major showers have been correlated with known comets confirms their cometary origin. Sporadic meteors are not in predictable orbits and represent cometary meteors that have had time to depart appreciably from the initial cometary orbits because of perturbing forces.

Asteroidal meteoroids are considered to be of different origin from the cometary meteoroids. Their origin is believed to be from the asteroids, a number of large masses (up to a 800-km diam) in orbit between Mars and Jupiter. As shown in a following section, the asteroidal meteoroids are of a much different structure from the typical cometary meteoroids. Their density is about an order of magnitude greater than that of the cometary meteoroids, and sometimes they are found to be 90 percent iron. In general, they are a compact stony type of particle, and frequently they survive the passage through the Earth's atmosphere and are found on the Earth's surface. Data are obtained

on the larger cometary (and very infrequently on the asteroidal) meteors by photographing the meteor trail.

Ideally, photographic meteor data supply four types of information: particle velocity, deceleration, trajectory, and photographic magnitude. These data are obtained by photographs of the meteor taken simultaneously with two Baker Super-Schmidt cameras for which the base line distance between them is accurately known (approx. 40 km). In each camera is a rotating shutter with a known period, and the area of the sky photographed by each camera is known (typically, 5980 sq km at a 90-km altitude). Unfortunately, not all the preceding information can be obtained for all meteors photographed with this equipment. The fainter meteors and those that do not have a complete trail on at least one of the plates cause complications in the determination of the particle characteristics. The fainter meteors have very short visible trails, which makes particle deceleration measurements virtually impossible.

From the photographic plates of a meteor that is bright enough and the trail of which is long enough, the velocity can be calculated by measuring the distance between breaks in the meteor trail caused by the rotating shutter. The deceleration is found by measuring the change in these distances between breaks, and the photographic magnitude is found by comparing the meteor brightness with the star background. Finally, each camera and the line of the meteor determine a plane in space containing the meteor path. The intersection of the two planes represents the meteor path in space. Extension of the planes allows the determination of the meteor trajectory (i. e., height and radiant) (ref. 7).

Basic Relations

An understanding of the physical equations governing the theoretical meteoric process is desirable in order to understand the procedure and assumptions made in calculating meteor densities and influx rates from the basic meteor data. Basically, these equations include conservation of momentum, conservation of energy, luminosity relation, and various combinations of these equations (ref. 8). In order to calculate meteoroid densities and influx rates, however, use of only the conservation of momentum and the luminosity relation are required. The equations presented are valid only for solid compact bodies traveling through the atmosphere. Fragmentation, or the breakup of the meteoroid as it passes through the atmosphere, complicates the use of these equations as shown in the following section.

Conservation of momentum. - Suppose that a compact meteoroid of mass m and density ρ_m enters the atmosphere with velocity v. (All symbols are defined in the appendix.) Air particles are trapped on or near the surface of the meteoroid, impart to it

the energy of collision, and decrease its forward momentum. The air particles are given a forward velocity while the meteoroid suffers a deceleration dv/dt; thus, by the principle of conservation of momentum,

$$m \frac{dv}{dt} = - \Gamma S \rho v^2 \tag{1}$$

where ρ is the density of the atmosphere, Γ is the particle drag coefficient, and S is the effective cross-sectional area of the meteoroid. One of the variables in equation (1) can be eliminated by expressing the effective cross-sectional area S as a function of the mass m. An assumption, however, must be made as to the shape of the meteoroid. If, for example, the meteoroid is a sphere of density ρ_m,

$$S = \left(\frac{9\pi}{16}\right)^{1/3} \rho_m^{-2/3} m^{2/3} \tag{2}$$

In general, the meteoroid is an irregularly shaped object, and the term $(9\pi/16)^{1/3}$ in equation (2) is replaced by a dimensionless shape factor A, which differs from body to body. With these transformations, equation (1) can be written as the first fundamental equation in meteor theory, called the drag equation:

$$\frac{dv}{dt} = -\Gamma A \rho_m^{-2/3} m^{-1/3} \rho v^2 \tag{3}$$

Luminosity relation. - The blackbody radiation from the surface of the meteoroid represents only a small fraction of the luminosity for the relatively small masses of the photographic or visual meteors under consideration. The principal source of the visual or photographic radiation occurs in a coma of vaporized meteoric material around and behind the meteoroid itself. Practically all the original energy is expended as the cloud of meteoric atoms collides with molecules of the atmosphere after the meteoric material has left the main body. The luminosity I is therefore assumed to be equal to the energy of the mass lost per second multiplied by a luminous efficiency factor τ. The luminosity is then expressed

$$I = - \frac{1}{2} \frac{dm}{dt} v^2 \tau \tag{4}$$

Thus, there are two basic equations, (3) and (4), with mass, velocity, and time as three variables; there are four unknown quantities: Γ, ρ_m, τ, and A. Two of the variables,

v and t, can be determined from photographic data, and the mass m is still to be found.

The integration of equation (4) yields

$$\int_{m}^{m_e} dm = \int_{t}^{t_e} \frac{-2I}{\tau v^2}\, dt \tag{5}$$

The terminal mass of the meteor can be shown to be nearly zero, so that

$$m = 2 \int_{t}^{t_e} \frac{I}{\tau v^2}\, dt \tag{6}$$

As shown in a following section, the luminous efficiency τ is related to a constant τ_o, called the luminosity coefficient, by the relation $\tau = \tau_o v$. Then,

$$m = \frac{2}{\tau_o} \int_{t}^{t_e} \frac{I}{v^3}\, dt \tag{7}$$

The mass referred to in equation (7) is the instantaneous mass at time t (the lower limit of the integral).

Substituting the mass from equation (7) into equation (3) and rearranging terms yields

$$\frac{\tau_o}{\rho_m^2} (\Gamma A)^3 = -2 \left(\frac{1}{\rho v^2} \frac{dv}{dt} \right)^3 \int_{t}^{t_e} \frac{I}{v^3}\, dt \tag{8}$$

Since the mass in equation (3) is an instantaneous value, this equation is valid at a point corresponding to the lower limit of the integral. The values of v, dv/dt, and ρ must be the values at this point corresponding to time t.

With these limitations, the right side of equation (8) can be determined from photographic data. The velocity, light intensity, deceleration, duration of the meteor, and atmospheric density (determined from the known particle height) are all measured quantities. In order to determine the density of the meteoroid, τ and ΓA must thus be determined (or, conversely, if ρ_m and ΓA are known, the luminous efficiency for a particular velocity can be determined). The preceding discussion indicates that meteoroid

densities can be calculated readily from equation (8) from photographic data along with estimated values of the luminous efficiency and the drag-area coefficient, as long as the meteoroids remain compact single bodies.

Fragmentation. - The typical meteoroid does not meet the conditions of compact body flight through the atmosphere. The development of a "correction factor" to be applied to the equations of compact meteor flight was therefore necessary. This correction factor, called the fragmentation index, was developed by Jacchia (ref. 9) as an answer to the "faint meteor anomaly." This anomaly was discovered when data from the more recent Baker Super-Schmidt cameras were compared with the predictions of the "ballistic" theory just presented. (The Baker Super-Schmidt cameras are capable of photographing much smaller, i.e., fainter, meteors than cameras previously used.) The durations of these meteors were shorter, and their decelerations increased more rapidly than predicted by theory.

These and other observed anomalies can be explained by the process of progressive fragmentation proposed by Jacchia. It is theorized that the meteor fragments progressively along its trail. Small fragments can be detached from the surface of larger meteor bodies without disrupting their unity, but if fragments of similar size are detached from small bodies, complete disruption into a cluster of fragments results. This phenomenon explains the higher frequency of occurrence of anomalies in the fainter meteor trails.

Jacchia developed a quantity, the fragmentation index, as a convenient measure of the progressive departure of the observed meteor deceleration from single-body theory. The fragmentation index χ is empirically determined and is defined as

$$\chi = \frac{d}{ds}\left(\log \frac{a_{obs}}{a_t}\right) \tag{9}$$

where a_{obs} is the observed acceleration, a_t is the acceleration computed from the drag equation (3), and s is the mass loss parameter, defined as

$$s = \log\left(\frac{m_\infty}{m} - 1\right) \tag{10}$$

where m_∞ is the original mass of the meteor before it entered the Earth's atmosphere, and m is the instantaneous mass of the meteor. Unfortunately, χ is not easy to determine, because it involves the second time derivative of the velocity; however, χ is approximately constant for each meteor during the detectable part of its flight (ref. 10).

The effect of fragmentation on equation (8) can be readily shown by rewriting equation (8) as

$$\frac{\tau_o}{\rho_m^2} = -2 \int_t^{t_e} \frac{I}{v^3}\, dt \left(\frac{\frac{dv}{dt}}{\Gamma A \rho v^2} \right)^3 \tag{11}$$

This equation was derived, as explained previously, by substituting a value for m into the drag equation. The drag equation gives the theoretical value for dv/dt; equations (8) and (11) are thus ideal or theoretical equations. In this idealized case, τ_o/ρ_m^2 remains a constant along the meteor's path (ref. 10), and, therefore, as long as consistent values of v, ρ, and dv/dt are used, the calculated values of τ_o/ρ_m^2 should remain the same. This implies that the observed value of acceleration a_{obs} is equal to the theoretical value of acceleration a_t (as given by the drag equation), and that the fragmentation index χ as seen from equation (9) is zero. In reality, equation (11) is

$$\left(\frac{\tau_o}{\rho_m^2} \right)_{obs} = -2 \int_t^{t_e} \frac{I}{v^3}\, dt \left(\frac{a_{obs}}{\Gamma A \rho v^2} \right)^3 \tag{12}$$

If the value of $\Gamma A \rho v^2$ from equation (3) is substituted, equation (12) becomes

$$\left(\frac{\tau_o}{\rho_m^2} \right)_{obs} = +2 \int_t^{t_e} \frac{I}{v^3}\, dt \left(\frac{1}{\rho_m^2 m} \right) \left(\frac{a_{obs}}{a_t} \right)^3 \tag{13}$$

If m is substituted in the idealized situation from equation (7),

$$\left(\frac{\tau_o}{\rho_m^2} \right)_{obs} = \left(\frac{\tau_o}{\rho_m^2} \right)_{ideal} \left(\frac{a_{obs}}{a_t} \right)^3 \tag{14}$$

Equation (14) further shows that if the observed acceleration equals the theoretical acceleration, $\left(\tau_o/\rho_m^2\right)_{obs}$ equals $\left(\tau_o/\rho_m^2\right)_{ideal}$, which is a constant.

Differentiating the logarithms of equation (14) yields

$$d \log \left(\frac{\tau_o}{\rho_m^2} \right)_{obs} = d \left[3 \log \left(\frac{a_{obs}}{a_t} \right) \right] \tag{15}$$

since $\left(\tau_o/\rho_m^2\right)_{ideal}$ is a constant for a given meteor. Substituting equation (9) into (15) yields

$$d \log\left(\frac{\tau_o}{\rho_m^2}\right)_{obs} = 3\chi \, ds \tag{16}$$

and integrating from s_o to s yields

$$\log\left(\frac{\tau_o}{\rho_m^2}\right)_{s_o} = \log\left(\frac{\tau_o}{\rho_m^2}\right)_{s} - 3\chi(s - s_o) \tag{17}$$

Equation (17) shows how two values of $\log\left(\tau_o/\rho_m^2\right)$ on the meteor trajectory corresponding to two values of the remaining meteoroid mass differ from one another. Again, in the absence of fragmentation ($\chi = 0$), the two values are the same.

The calculated value of $\log\left(\tau_o/\rho_m^2\right)$ for any meteor can now be related to some reference point corresponding to s_o. The data, to be most significant, should be reduced to the value of s_o corresponding to the beginning of fragmentation. Unfortunately, this value is not generally known, and the data are corrected to a value of s near the beginning of the meteor. It is indicated intuitively, that the fragmentation index is also an index of credibility; that is, the data from meteors with very little fragmentation are "corrected" by the least amount and represent data that deviate the least from theoretical considerations.

An excellent example of the use of photographic meteor data with the fragmentation correction is given by Verniani (ref. 10). Also discussed is a system of "weights" by which the calculated values of $\log\left(\tau_o/\rho_m^2\right)$ at different values of s along the meteor trajectory are deemed credible or not.

With the introduction of the fragmentation correction, it is now generally possible to use equation (11) to determine meteoroid density if the luminous efficiency τ and the drag-area coefficient ΓA are known.

Luminous efficiency. - The numerical value of the luminous efficiency τ is perhaps the largest single influencing factor in the reduction of meteor data. Estimates of τ appearing in the literature have differed from one another by as much as two orders of magnitude. Öpik (ref. 11) has offered a theoretical evaluation of τ for both solid and dust-ball photographic meteors. His analysis is lengthy and involved, and by far the most complete work to date. The analysis calculates the radiation energy emitted in the wavelength range 4500 to 5700 Å by iron atoms in a cloud through which a stream of nitrogen

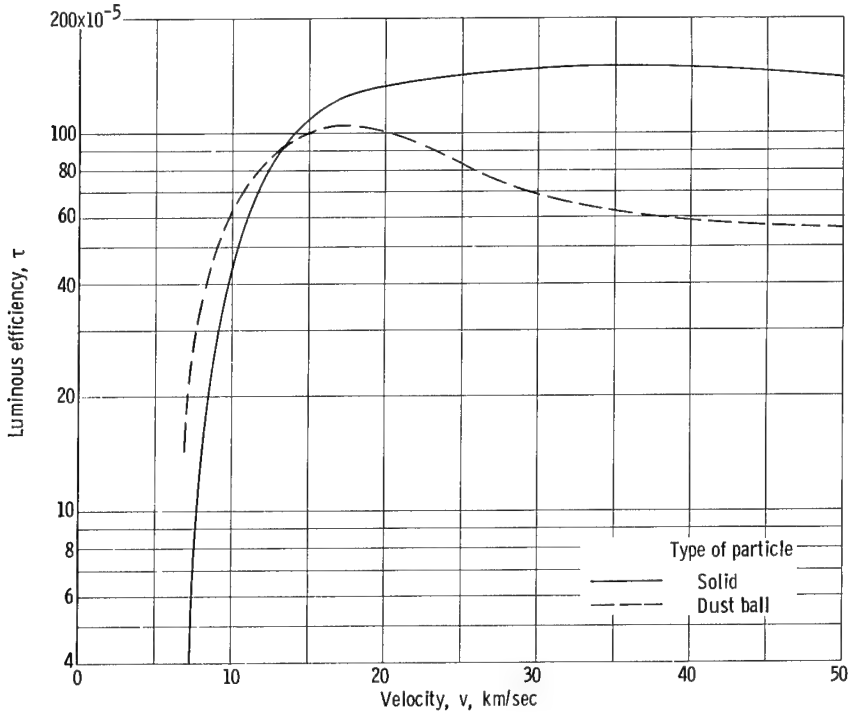

Figure 1. - Variation of theoretical luminous efficiency with velocity according to Öpik (ref. 11).

atoms is moving with a series of specific high velocities. For the diluted coma condition (dust ball), he assumed that the physical process is better represented by single iron atoms moving through a cloud of nitrogen atoms, which he shows produces less total radiation energy.

The results of Öpik's work are shown in figure 1, in which luminous efficiency is plotted as a function of meteor velocity relative to the Earth. Note the radical dependence of τ on velocity at values less than 15 kilometers per second. Öpik's work predicts a value of zero for luminous efficiency at velocities less than 5.2 kilometers per second. At high velocities, however, the luminous efficiency is very nearly constant for both the solid particle and the dust ball. Öpik's theoretical values have been used quite extensively by investigators in the field of meteor astronomy (e.g., refs. 12 and 13).

An attempt has recently been made to measure the luminous efficiency of an artificial iron meteor of known mass and density (ref. 14). In this experiment, a seven-stage rocket (Trailblazer I) was employed to accelerate a stainless-steel projectile of approximately 2.2 grams into the atmosphere at 10 kilometers per second. The entry of the projectile was recorded photographically, and methods of photographic reduction, well documented (e.g., ref. 7), were employed to obtain the luminous efficiency for iron meteors. This value was further reduced to the efficiency of stony particles by assuming that the stony particle was 15 percent iron and that all the visible light given off was due to iron (ref. 11). This value is then assumed typical of meteoroids that are, for the lack

of better information, assumed stony in composition.

As another source of data, values of luminous efficiency for three photographed asteroidal meteors were calculated by Cook, Jacchia, and McCrosky (ref. 15). Two of the meteors were assumed to be stone. The other was identified to be pure iron from its available spectrum. Because of the assumed compact nature of the asteroidal particles (as opposed to the "fluffy" cometary particles), a good approximation to their density was made and the luminous efficiency was calculated with a fair degree of confidence. The results of these calculations for the asteroidal particles are shown in figure 2 along with the value obtained from the Trailblazer experiment. Fairly good agreement with Öpik's theoretical calculation for a solid particle is seen. Unfortunately, however, all these experimental points are in the low-velocity range of the curve and do not prove, or disprove, the constancy of τ at high velocities (>20 km/sec) for this type of particle.

Most investigators have recognized the dependence of the luminous efficiency of a cometary meteor upon its velocity. In general, for analytical purposes, an equation of the form

$$\tau = \tau_0 v^n \tag{18}$$

is used to describe this dependence, where τ is the luminous efficiency, τ_0 is a constant (luminosity coefficient), and v is the meteoroid velocity. The exponent n is believed to be somewhat less than one (ref. 16). For simplicity in calculation, however, and because of the fact that the experimental data can reasonably be fitted within its range of error, most investigators use 1 for the exponent n; that is,

$$\tau = \tau_0 v \tag{19}$$

Shown also on figure 2 is the analytical curve for τ according to equation (19) where $\tau_0 = 10^{-19.42}$ (units of zero magnitude (visual) $g^{-1}cm^{-3}sec^4$), given by Whipple as the best estimate for use in his calculations (ref. 17).

Recently, Verniani (ref. 10) made an extensive evaluation of the value of n and of the absolute value of τ_0 for cometary meteors. His analysis used 400 precisely reduced meteors and represents the first attempt to analyze existing data on cometary meteors for this purpose. His analysis takes fragmentation into account and is based on a knowledge of average meteoroid density. Also, as indicated in the next section, his analysis treated so large a sampling of meteors that the effects of unknown individual values of the drag-shape factor were reduced. Furthermore, he indicated that $n = 1$ is a good representation of the luminosity law over the complete range of meteor velocities (10 to 72 km/sec). It is indicated from the analysis that a linear relation between luminous efficiency and velocity (eq. (19)) may be a better representation of the luminosity

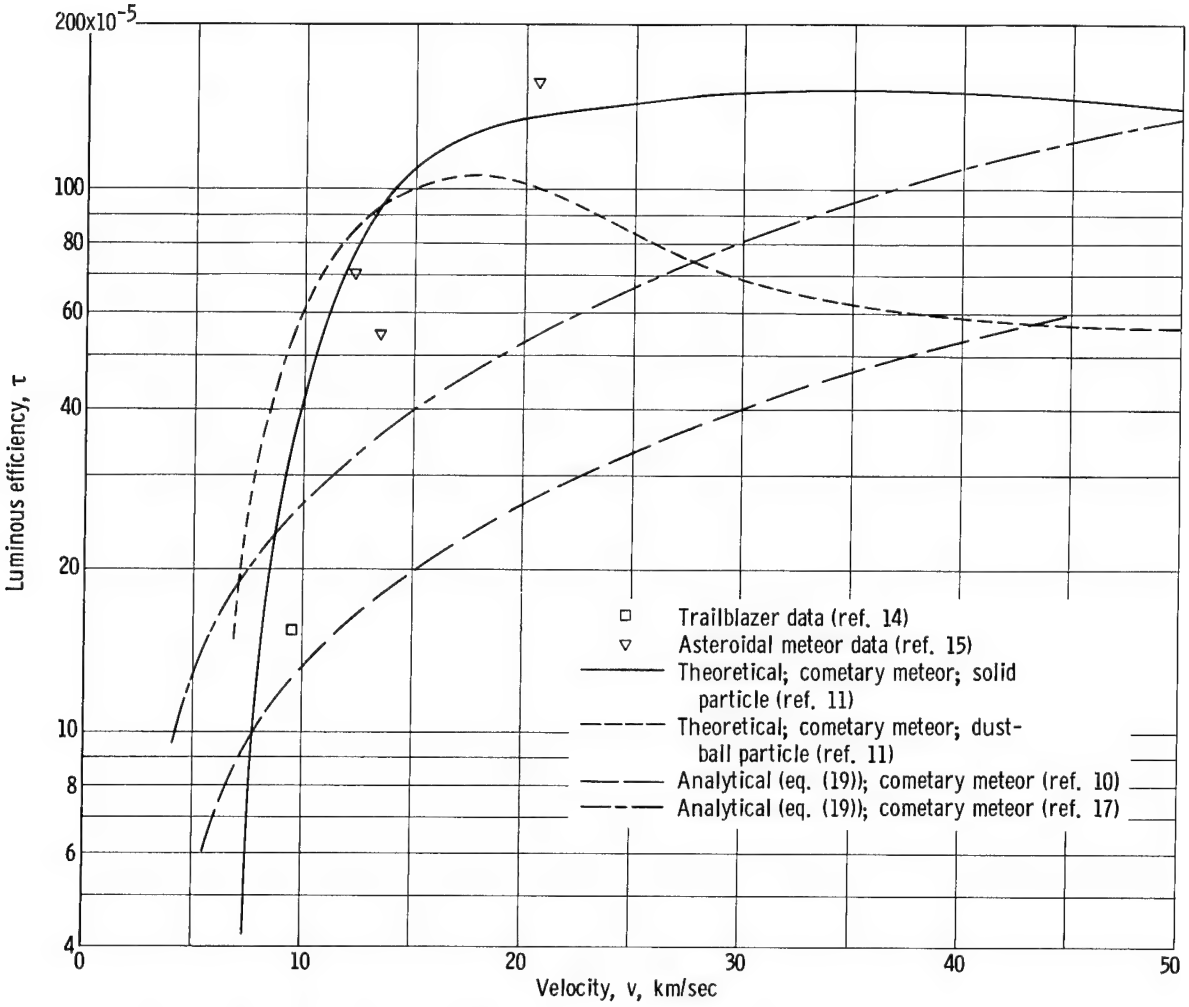

Figure 2. - Luminous efficiency as function of velocity. Comparison of theoretical, experimental, and analytical variations.

law for cometary meteors than that proposed by Öpik's dust-ball curve. The analytical variation for τ obtained from Verniani is also shown in figure 2.

Drag-shape factor ΓA. - The particle drag coefficient Γ has been shown to be approximately equal to 1 in free molecular flow and approximately 1/2 in continuum flow (ref. 16). Levin (ref. 8) has shown that Γ should assume values of 0.5 to 1.1 for conditions of meteor flight most likely to be encountered. Conditions for typical photographic meteors are best represented by $\Gamma = 1.1$ (free molecular flow) (ref. 10). For the larger asteroidal meteors, the conditions of continuum flow prevail with $\Gamma = 0.5$.

The dimensionless shape factor A, as defined in equation (2), is a function of the shape of the meteoroid. For a sphere, $A = 1.208$, and for a cube traveling with one face normal to the direction of motion, $A = 1.00$. For an oblate spheroid with the minor axis in the direction of flight,

$$A = \left(\frac{9\pi}{16b^2}\right)^{1/3} \tag{20}$$

where b is the ratio of the minor to the major axis. Realistic estimates of A based on experimental data are impossible to obtain. Probable limiting values of A are difficult to determine since a meteoroid can be conceived to have a shape ranging from a long rodlike structure to a platelike structure.

Experimentally, Cook, Jacchia, and McCrosky (ref. 15) found that if $\Gamma A = 0.92$, the average luminosity coefficient of the three asteroidal meteors would be in agreement with the Trailblazer (artificial meteor) experiment. The values of the luminous efficiency for the three asteroidal particles plotted in figure 2 were calculated by assuming each was a sphere ($A = 1.208$). An average value for the luminosity coefficient for the three meteors was calculated based on the linear dependence of τ on v in equation (19), and this value was then compared with the luminosity coefficient derived from the Trailblazer experiment. By adjusting the drag-shape factor of the average asteroidal meteor to 0.92, exact agreement between the derived luminosity coefficients of Trailblazer and the asteroidal meteor average was found, and the average value for A was 1.84. This value implies that the "average" shape of the associated asteroidal meteors treated was an oblate spheroid with the major axis about 1.9 times the minor axis.

In treating a large sample of cometary meteor data, Verniani (ref. 10) indicated that the assumption of the meteoroid as a sphere ($A = 1.208$) is a good estimate since the shape-factor effect will average out if the meteoroid shapes are assumed to be entirely random.[1] Individual calculations of meteoroid density and luminous efficiency are, therefore, only as good as the estimated value of the shape factor. For a large sample

[1]This assumption may represent a lower limit for A, since a sphere has the least ratio of mass to surface area of any solid object.

treated as a whole, however, the effects of values of A differing from that of a sphere are assumed to "average" out, but for individual cases, gross errors in the calculated results are possible.

METEOROID CHARACTERISTICS

Density

Until recently, the average density of meteoroids was assumed to be the same as the average density of meteorites.[2] This assumption led the astronomer to believe meteoroids were stony iron or iron in nature with a density in the range of 3.5 to 8.0 grams per cubic centimeter. With this assumption of meteoroid densities, investigators in the field of meteor astronomy were able to calculate atmospheric densities from photographic meteor data. With the onset of rocketry came direct measurement of the atmospheric density profile at altitudes previously calculated from meteor data. Comparison of the calculated and measured values of atmospheric density showed that the calculated values were consistently low in the altitude range above 75 kilometers. This discrepancy of values could be resolved if the density of meteoroids were assumed to be much lower than that previously used. Whipple (ref. 18), through his icy-conglomerate comet model, proposed just such a low-density fragile structure for an average meteoroid of cometary origin. Öpik was also a proponent of the fragile-structure school of thought. His concept differs slightly from that of Whipple in that he proposed that the cometary particles entering the Earth's atmosphere and producing meteors are dust balls composed of a great number of individual grains (refs. 19 and 20). In effect, both models imply a low overall bulk density for a cometary meteoroid.

Whipple (ref. 13) and others then reversed the process of calculation by assuming atmospheric densities to be known and meteor densities to be unknown. This procedure, with improved estimates of the constants involved in the physical equations of meteor phenomena and recognition of meteor fragmentation, is the one used today. Reevaluation of meteoroid densities based on this reversal in calculation led to the proposed low bulk density of a meteoroid.

Whipple, in his latest work (ref. 17), has done this for a group of meteors previously reduced by Jacchia (ref. 12). As explained previously, the right side of equation (8) is a function only of the photographic data and atmospheric density. Whipple refers to this value as K^{-3}. Thus, from equation (8),

[2]A meteoroid is a particle in space; a meteorite is a meteoroid that has survived the passage through the Earth's atmosphere and has impacted the Earth. Meteorites are generally believed to be asteroidal in origin.

$$\frac{\tau_o}{2\rho_m^2}(\Gamma A)^3 = -\left(\frac{1}{\rho v^2}\frac{dv}{dt}\right)^3 \int_t^{t_e} \frac{I}{v^3}\,dt \equiv K^{-3} \tag{21}$$

From the data of reference 12, Whipple obtained an average value of the right side of equation (21) based on 88 meteor cases. The value of $K = 10^{6.37}$ (units of zero magnitude (visual) $g^{-3}cm^{-5}sec^4$) together with the values of $\tau_o = 10^{-19.42}$ and $\Gamma A = 0.92$ led Whipple to conclude that the typical photographic meteor density is 0.44 gram per cubic centimeter.

There seems to be an inconsistency in the values and therefore in the proposed density of reference 17. The value of $\tau_o = 10^{-19.42}$ is a logarithmic average of the value of τ_o determined from the asteroidal particles in reference 15 and the value of τ_o determined from the Trailblazer experiment (ref. 14). These values were determined with the assumption of $\Gamma A = 0.6$ (corresponding to a sphere with $\Gamma = 1/2$). As explained previously, if $\Gamma A = 0.92$ is assumed for the asteroidal particles, the values of τ_o for the Trailblazer and the asteroidal particles could be made to agree. It therefore seems that if the logarithmic average of τ_o is employed, the value of $\Gamma A = 0.6$ must necessarily be used, or if $\Gamma A = 0.92$ is to be used, the value of τ_o for the asteroidal particles and the value of τ_o for the Trailblazer experiment must agree with one another and no averaging is necessary. Apparently Whipple recognized this inconsistency because, on page 29 of reference 17 he states that a better value of τ_o is $10^{-19.63}$, with $\Gamma A = 0.92$. These latter values are consistent with the results of reference 15. Employing these latter values, Whipple revised his best estimate of meteoroid density to 0.25 gram per cubic centimeter.

Verniani (refs. 10 and 21) recently made an exhaustive study of a total of 700 meteor cases in order to define meteoroid densities. In reference 10, equation (8) is applied to unpublished data obtained by Jacchia. The 359 cases treated in this reference had measured decelerations that made the use of equation (8) possible. The meteors were corrected for fragmentation, and the atmospheric density for application in the right side of equation (8) was determined from the known height of the meteor. Since each meteor was assumed to be a sphere, $\Gamma A = 1.3$, and Verniani's derived value of $\tau_o = 10^{-19.72}$ was used.

The results of Verniani's calculations are shown in table I. These average values are believed to be significant because of the application of the spherical shape factor, which, as explained previously, is assumed to be a valid assumption when applied to a large sample. Table I groups the meteors into subsamples of all sporadic meteors, sporadic meteors with the aphelion distance Q less than 7 astronomical units, sporadic meteors with the aphelion distance greater than 7 astronomical units, and the various

TABLE I. - DENSITY OF METEORS COMPUTED BY USE OF DRAG EQUATION (REF. 21) FROM UNPUBLISHED DATA

Meteor	Number	Density, g/cu cm
All sporadic meteors	247	0.21
Sporadic meteors with aphelion distance $Q < 7$ AU	155	.23
Sporadic meteors with aphelion distance $Q > 7$ AU	92	.16
Taurids	23	.20
Geminids	20	.92
Aquarids	16	.24
α Capricornids	13	.12
Quadrantids	9	.15
Perseids	9	.28
Orionids	8	.14
η Cygnids	4	.14
Lyrids	3	.28
σ Hydrids	3	.30
Virginids	2	~.70
Draconids	2	~.001
Total	359	

identifiable showers. The separation of the sporadic meteors into these two groups is an attempt to show the differences between long- and short-period meteors by defining arbitrarily an aphelion distance of 7 astronomical units as the dividing line. The results show that the density is generally smaller than 0.44 gram per cubic centimeter, with the average of all the sporadic meteors slightly greater than 0.2 gram per cubic centimeter. This value agrees with the results as finally derived in reference 17 of an average density of 0.25 gram per cubic centimeter.

The short-period meteors have a density about 20 percent greater than the long-period meteors. Also, the density of shower meteors with small orbits (Geminids, Taurids, Quadrantids, and Aquarids) is, on the average, larger than that of showers with elongated orbits (Orionids and Perseids). The significance of this difference between long- and short-period meteor densities is uncertain. Some investigators believe that the short-period meteors have as their origin the inner core of the comet. The short-period comet is, on the average, closer to the Sun than the long-period comet and will disintegrate more rapidly. The long-period meteors, however, originate from the outer surfaces of the long-period comet and may be less compact.

A search among the meteors studied in this sample revealed no dependence of the density on mass or photographic magnitude (ref. 21). Furthermore, the meteors used by Whipple (ref. 17) from which he obtained a density of 0.25 gram per cubic centimeter

TABLE II. - DENSITY OF METEORS COMPUTED BY APPROXIMATE GROUP METHOD OF CALCULATION (REF. 21) FROM PHOTOGRAPHIC DATA OF REFERENCE 24

Meteor	Number	Density, g/cu cm
All sporadic meteors	280	0.22
Sporadic meteors with aphelion distance $Q < 7$ AU	203	.23
Sporadic meteors with aphelion distance $Q > 7$ AU	77	.19
Taurids	17	.17
Geminids	16	.32
Aquarids	10	.49
Orionids	12	.18
Perseids	9	.14
Quadrantids	5	.27
Bielids	2	~.35
α Capricornids	2	~.10
Monocerotids	1	~.20
Draconids	1	~.001
Total	355	

are of a much greater average mass than those used in reference 21, which produced a density of 0.2 gram per cubic centimeter. This range of mass in which essentially no dependence of density on mass was found is approximately from 100 to 10^{-2} grams, or four orders of magnitude.

As pointed out previously, it is not always possible to determine meteoroid deceleration from photographic plates. This difficulty often makes using equation (8) impossible for determining meteoroid density. In reference 21 an approximate method is developed for determining meteoroid densities that does not require meteor deceleration but rather meteor height at maximum light intensity. The method relates the meteor's shape, mass, and density to the atmospheric pressure at maximum light by making certain assumptions as to the physical strength of the meteor. It is indicated that the method is approximate and valid only when applied to a large group of meteors. The method, as derived, gives average density directly and loses meaning when applied to single cases.

For comparison purposes, table II lists values of average density for a group of 355 meteors (from ref. 21) calculated by this method. The values calculated by this method are in close agreement with the direct calculations shown in table I for the sporadic meteors. As is to be expected, the showers calculated by the two different methods do not show good agreement with one another when the sample size is small. These results indicate an average value of meteoroid density typical for sporadic meteors to be about 0.2 gram per cubic centimeter.

Structure

As mentioned in the preceding section, meteors, irrespective of size, were earlier thought to be compact stones or iron chunks. With better knowledge of the upper atmosphere and observations of visual and photographic meteors, it was recognized that all meteoroids could not have such a high density. Reinterpretation of the photographic meteor data, as explained in the preceding section, has led to the belief that meteoroids may have a bulk density of about 0.2 gram per cubic centimeter. Furthermore, photographic data indicate that most meteors break up at the high altitudes at which they first appear. Öpik (ref. 11) indicates that the visible meteors typically have a crushing strength of about 10^4 dynes per square centimeter (0.145 lb/sq in.), or about the crushing strength of cigar ash. The structure and composition of meteoroids are therefore also important considerations.

The spectra of many meteors have been obtained (ref. 4), but no specific percentage compositions are reported. The occurrence of the lines of specific elements in the meteor spectra analyzed, however, is given. The presence of the following elements has been detected: sodium, potassium, silicon, aluminum, magnesium, calcium, manganese, chromium, and iron (ref. 22). Calcium and iron have been recognized as the two most prevalent elements in meteor spectra. These data, however, do not allow any conclusions regarding the typical cometary composition because of their qualitative nature. In order to obtain quantitative meteor spectra, the luminous efficiency of each element in the spectrum must be known.

McCrosky and Soberman (ref. 14) have indicated another means for estimating the composition of typical cometary meteoroids. The relative ratio of heavy elements to oxygen in stony meteorites is approximately the same as the relative ratio of heavy elements to oxygen in the Sun. Since the meteor spectra indicate the presence of these heavier elements, the assumption is made that the same relative ratio of heavy elements to oxygen exists in the typical cometary meteoroid as in the Sun and in stony meteorites (ref. 14). For this reason it has been concluded that the typical meteor is "stony" in composition.

The observed data indicate then that typically a meteor appears at high altitudes (from which low density and low crushing strength is inferred), and the assumption is made that its composition is typically stony. The meteoroid structure proposed must necessarily produce phenomena in agreement with the observed data and assumptions.

Two possible explanations exist for the observed phenomena: the first is drag distortion and the second is the "dust-ball" concept of a meteoroid. Under the drag-distortion interpretation, a compact stony meteoroid entering the atmosphere melts because of friction into a spherical drop. Atmospheric drag causes the meteor to flatten out into an oblate spheroid with its minor axis in the direction of flight. The increased

ablation cross section (frontal area) would then cause the meteor to appear at extremely low atmospheric densities. Öpik (ref. 11), however, shows that for compact meteors under the influence of drag distortion, the length of the meteor trail should decrease with increasing brightness. No such effect has been observed statistically, and he therefore concludes that the explanation of the increased area of ablation as an effect of deformation of a drop is not acceptable. If, then, the compact meteor model deforming under drag distortion is discarded, the acceptance of low bulk density, low crushing strength, and stony composition as typical of photographic meteors is necessary. It is easy to visualize this type of particle as being constructed like a cigar ash with layers of soft, loosely bound material, or as a stony sponge.

These cigar ash or stony spongelike particles could have the comets as their origin as proposed in the icy-conglomerate comet model of reference 18. In essence, the proposal is that the comet can be thought of as a large frozen-gas snowball interlaced with either the stony sponge or cigar ash material presented previously. Upon repetitive passage in proximity to the Sun, the gases boil off and leave the porous, fragile, low bulk density material on the outer surface of the comet. Solar radiation, internal pressures, and thermal shocks cause the outer surface of the comet to break up into the meteoroids observed as meteors. This particular model of meteoroid formation seems to propose a particle that satisfies the observed phenomena.

As mentioned previously, Öpik also proposed a meteoroid model to meet the requirements of low density and low crushing strength (refs. 19 and 20). He proposed a model in which the meteoroid is composed of a great number of individual compact grains loosely held together; however, he offers no detailed explanation of the injection mechanisms of such a particle. The differences between Öpik's dust-ball meteoroids and Whipple's cometary particles are insignificant, and one could justify the same type of origin for the dust ball. In effect, the three meteoroid structures previously discussed could be grouped as one: cometary dust balls.

An interesting proposition has been offered by Donn (ref. 23) for the origin of meteoroids that would give them a somewhat different type of construction. In that reference, it is surmised that original meteoroid grains were condensed from the primordial gas of the solar nebula when the planets were formed. The grains then agglomerated with a volatile binding material to form comets. The method of injection of these cometary grains into meteoritic particles then is the same as that proposed by the icy-conglomerate comet model.

The significant contributions of the theory of reference 23 is in the proposed structure of the cometary meteoroid. It is shown that the particles formed by primordial gas condensation would grow as whiskers, filaments, platelets, or some combination resulting in a complex, irregular structure. The original particle can then be described as a steel-wool type of structure as one possibility or a many-pointed starlike structure as

another. The platelet structure would again propose the ashlike conglomerate. Very little change in the original particle structure would result from cometary agglomeration, and thus the cometary particles of today would have very nearly preserved the primordial condensate structure and composition they originally possessed (ref. 23). This theory of meteoroid structure would again fulfill the observed low crushing strength and low density typical of photographic meteoroid particles.

All the previously discussed possible structures for typical cometary meteoroids have two characteristics in common: distributed mass with low bulk density and low crushing strength. The question then arises as to the impact damage capabilities of this type of particle. Existing experimental hypervelocity impact data indicate a very weak relation between penetration and particle density $\left(P \propto \rho_m^{1/6}\right)$ (e.g., ref. 1). These existing data, however, were obtained with solid homogeneous projectiles and the density-damage relation for heterogeneous, low bulk density type particles is unknown. Furthermore, the effect of the low crushing strength of the meteoroid on penetration damage is also unknown. Again, all experimental and theoretical penetration data to date have been obtained with projectiles, the crushing strength of which is orders of magnitude higher than the speculated crushing strength of the typical cometary meteoroid. In general, low bulk density and low crushing strength in a heterogeneous particle are codependent, and thus the individual effects are not likely to be separated.

Velocity

A knowledge of meteoroid velocities, besides being required for meteor data reduction purposes, is necessary as an input for design protection calculations (ref. 1). Ideally, a spatial velocity distribution may exist for meteoroids. To date, a spatial velocity distribution curve has not been developed. For this reason, "average" meteoroid velocities have been proposed. It must be remembered, however, that this average velocity proposal is the velocity relative to the Earth and not necessarily the "impact" velocity, or velocity relative to the space vehicle in question. For these reasons a discussion of meteoroid average velocities is felt necessary.

Figure 3(a) presents a velocity histogram of 285 sporadic meteor cases as reported by Hawkins and Southworth (ref. 24). The velocities are relative to the Earth at the upper limit of the atmosphere. These data are significant to study since, as discussed in a following section, they are the data used by Whipple in proposing his latest influx rates (ref. 17). The distribution of these sporadic data is bimodal and shows a peak at a velocity of about 20 kilometers per second and another at about 67 kilometers per second. The reduced values between 45 and 55 kilometers per second represent meteors in relatively unlikely orbits as explained in reference 24.

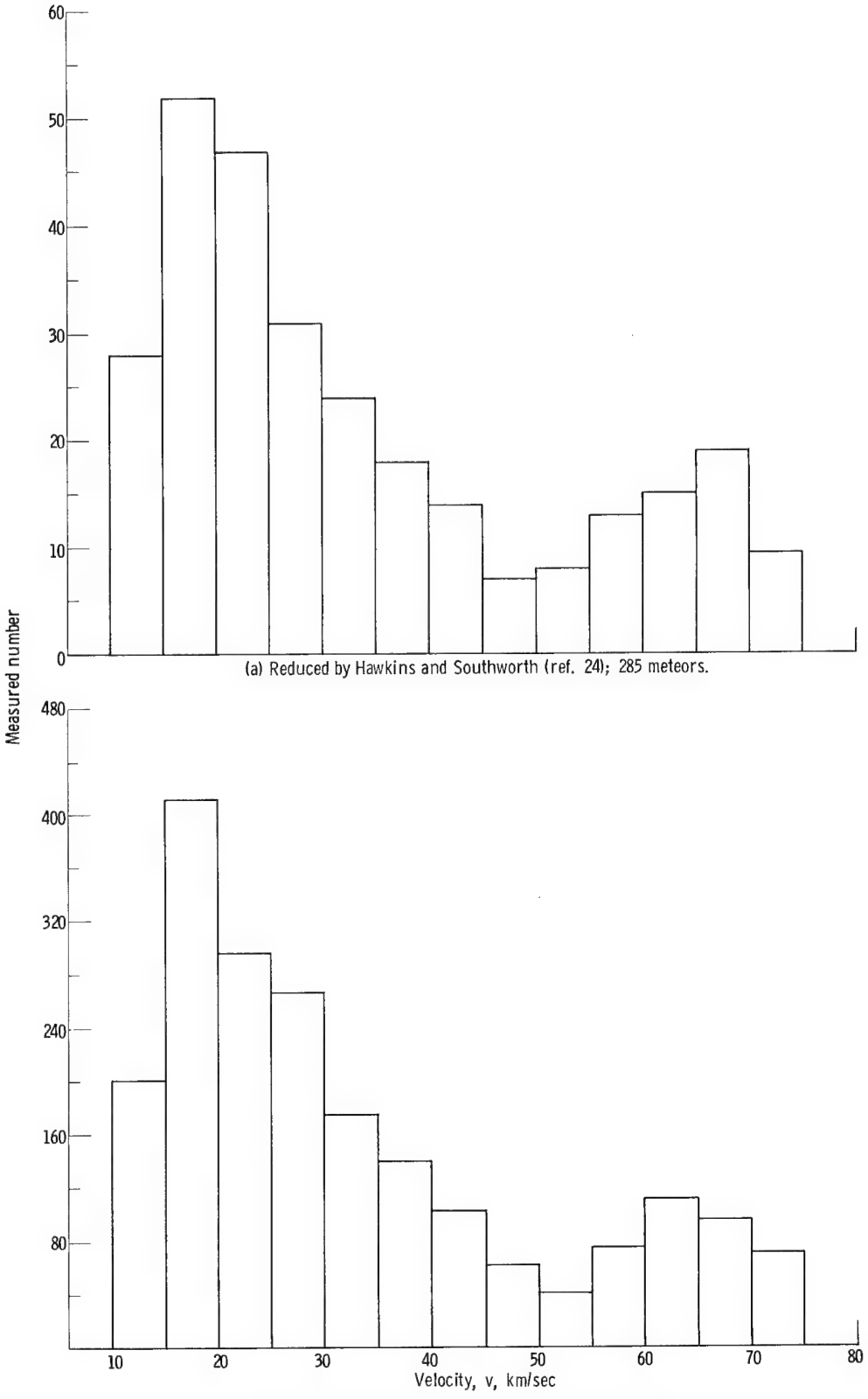

(a) Reduced by Hawkins and Southworth (ref. 24); 285 meteors.

(b) Reduced by McCrosky and Posen (ref. 25); 2048 meteors.

Figure 3. - Velocity histograms for sporadic meteors. Average velocity, 30 kilometers per second.

A velocity histogram derived from the data of McCrosky and Posen (ref. 25) is shown in figure 3(b). The data consist of 2048 meteor cases that were determined to be sporadic. The virtual agreement of the two histograms thus verifies the randomness of the data. As indicated in reference 25, the method of reduction used for these latter data is not so accurate as the method used in reference 24. The randomness of the errors, however, validates the treatment of the sample as a group.

An arithmetic average of the two histograms yields approximately 30 kilometers per second for both the data of reference 24 and those of reference 25. This value of average meteoroid velocity (relative to the Earth) has frequently been used for the impact velocity in meteoroid protection calculations.

The average velocity obtained from figure 3 represents an average velocity of the observed sample. The observed velocity distribution, however, is not considered to be representative of the true velocity distribution in space because of a velocity bias of observation. Such a bias exists because, in general, it is easier to "see" the high-velocity meteors because they produce brighter trails; that is, relatively more of the existing meteors are observed when their velocities are high.

As indicated in reference 25, the velocity bias of observation on a photographic plate is the combination of two effects. The first effect is seen from equation (4), with $\tau = \tau_0 v$. This relation indicates that the light intensity per unit time from a meteor of a particular mass is a function of the cube of its velocity. Comparison of light energies emitted by individual meteors proportional to the ratio of the cube of their velocities is exact, however, only when the masses and duration times are equal (i. e., when dm/dt is constant).

The second factor contributing to the velocity bias of observation arises from the effective exposure time on the photographic plate. The plate exposure time is an inverse function of the translational velocity of the point source; therefore, the intensity of light recorded on the plate is also inversely proportional to the source velocity. This exposure-time effect will influence the observed velocity histograms in a manner opposite to that of the previous velocity-energy effect, since the faster the meteor travels, the less it is exposed on the photographic plate. The velocity histograms are thus weighted in the direction of the low-velocity meteors. In reality, however, the situation is not quite so simple, since the meteor does not emit light energy as a traveling point source. In theory, the visible light energy is emitted by excited meteoric mass particles caused by high-energy collisions. These excited particles trail the meteoroid by some finite distance and emit as a large number of point sources. The exact dependence of exposure time on meteor velocity is further complicated by the existence of a directional variation of the velocity vector of the meteor with respect to the photographic plate and by the variation in meteor range. (High-velocity meteors have, statistically, a greater range.)

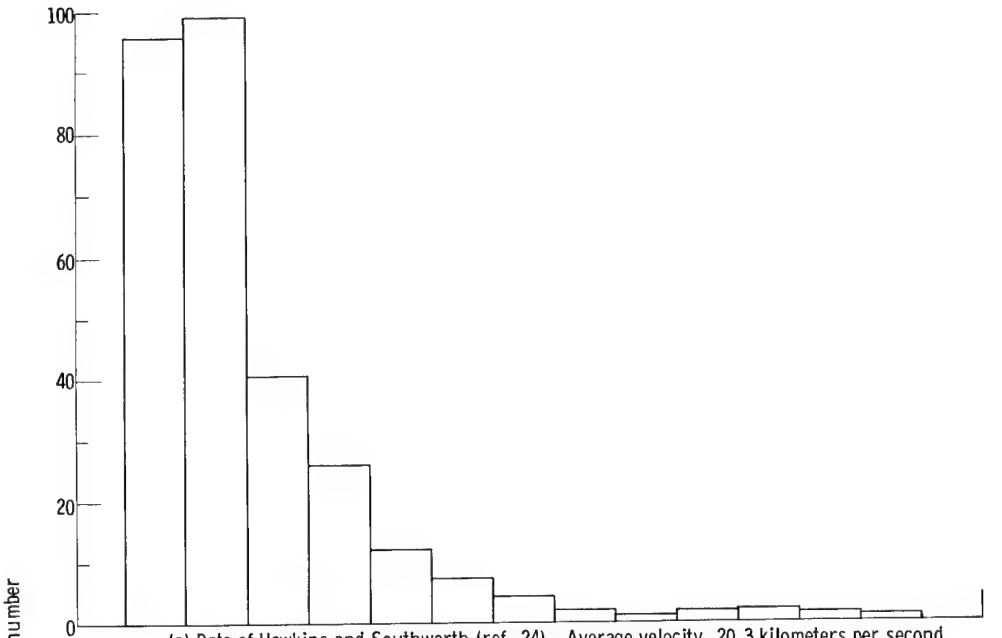

(a) Data of Hawkins and Southworth (ref. 24). Average velocity, 20.3 kilometers per second.

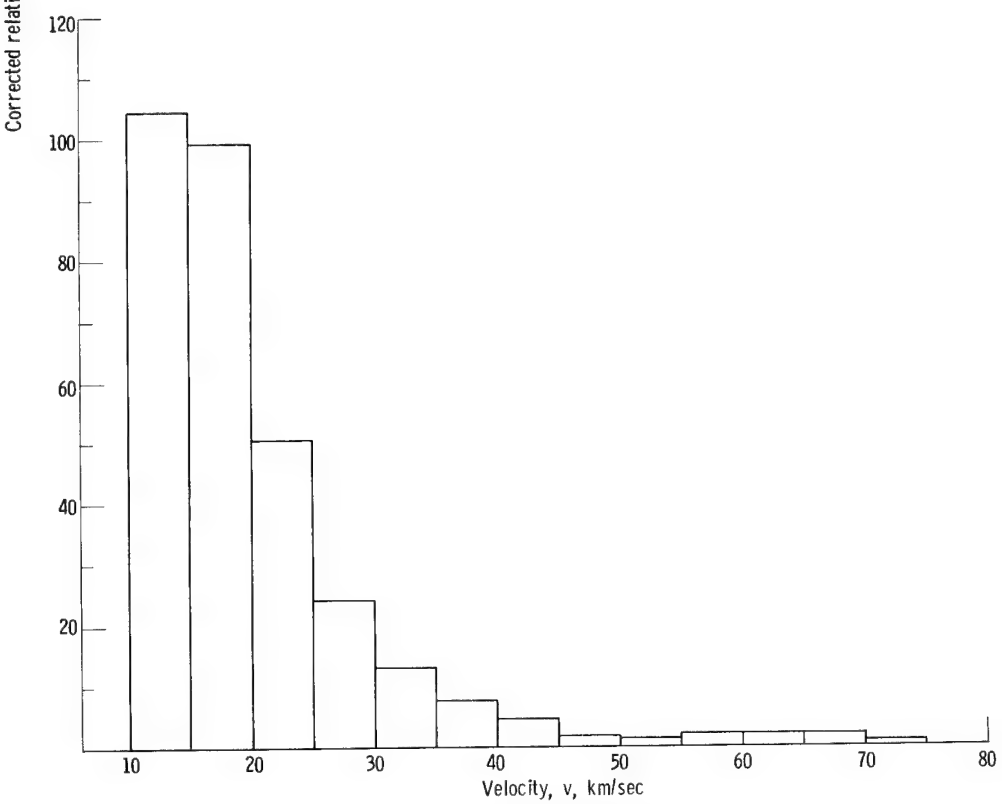

(b) Data of McCrosky and Posen (ref. 25). Average velocity, 20.2 kilometers per second.

Figure 4. - Corrected velocity histograms.

The exact observational bias function can be calculated only for individual cases and is quite involved. An approximate velocity bias for large samples, however, may be chosen as proportional to $1/v^2$ by combining the preceding two effects as recommended in reference 25. The observed count is then adjusted for this effect. In accepting this relation for the removal of the velocity bias of the histograms of figure 3, it must be assumed that, in the photographic mass range of interest (10^{-2} to 10^{0} g), there is no pronounced dependence of meteoroid velocity on mass. The further assumption is made that these histograms are representative of any small mass range within the limits of 10^{-2} to 10^{0} gram. Then, for this "constant-mass" histogram there is a higher probability of observing the high-velocity particles than the low-velocity particles.

In establishing a more nearly correct count, it is assumed that all existing particles are observed for velocities between 70 and 75 kilometers per second in figure 3, and a correction for the velocity bias of the photographic observations proportional to $1/v^2$ is made for the other velocity ranges. On this basis, the "true" distribution of particle velocities for the samples considered assume the shapes shown in figure 4. As expected, these histograms indicate many "unobserved" particles of low velocity, and significantly this indicates that there is more flux present than observed. The average velocity of the true distribution of the data of reference 24 (fig. 4(a)) is 20.2 kilometers per second and of the data of reference 25 (fig. 4(b)) is 20.3 kilometers per second, values that are significantly less than the nominal 30 kilometers per second of the "observed" distributions.

MASS INFLUX RATE

The design engineer must know how many meteoroids of a particular mass will be encountered by the vehicle during its trajectory. The determination of meteoroid influx rates from photographic meteor data has been thoroughly treated by Hawkins and Upton (ref. 26). The classical approach employed in reference 26 is generally accepted and will be briefly explained herein. The photographic data obtained, as explained previously, yield the light intensity and photographic magnitude of the meteor directly. An examination of these data shows an increase in the number of the faint meteors as compared with the bright meteors, which indicates an increase in the number of meteors with decreasing mass.

Hawkins and Upton (ref. 26), from a random sample of 285 sporadic meteor trails, derived an equation for the cumulative influx rate N, expressed as a function of the photographic magnitude M_p over the range of photographic magnitudes from -2.0 to +4.0, in the form

$$\log N = aM_p - \log N_0 \tag{22}$$

where the constant a is the slope of the curve of log N against M_p and N_0 is the number of meteors with magnitudes equal to or less than zero. Here, the photographic magnitude M_p is an average value over the meteor trail. By simply counting the number of meteors with magnitudes less than or equal to zero, log N_0 was determined:

$$\log N_0 = -4.34 \tag{23}$$

(where N_0 is in $km^{-2}hr^{-1}$). This number was based on an average rate of observation by the viewing cameras of 0.278 meteor per hour over a collection area of 5980 square kilometers of sky. The number of meteors increased by a factor of 3.4 per magnitude and thus produced a value of a of 0.537. Equation (22) then becomes

$$\log N = 0.537\, M_p - 4.34 \tag{24}$$

The representation of meteor flux rate in terms of photographic magnitude given by equation (24) is perhaps the most accurate form of this type of information. It is uncontaminated by further calculations and is strictly a derived representation of raw data. The accuracy of the equation is a function only of the accuracy of measurement of the photographic magnitude and the area of the sky photographed. This representation of meteoroid influx rate, however, is not very usable for space-vehicle-protection requirements, since a knowledge of meteoroid mass-influx rates is necessary.

Hawkins and Upton Rate

Hawkins and Upton (ref. 26) indicate that they also calculated individual masses for each sporadic meteor in their sample of 285 sporadic meteors. This calculation can be made, as explained previously, by the use of equation (7) with an assumed value of the luminosity coefficient. The choice of a particular value for the luminosity coefficient then implies that a consistent value of an average meteoroid density is determined. This value is approximately 3 grams per cubic centimeter for the influx rate of Hawkins and Upton. They found that the cumulative influx rate N could be expressed as a function of the meteoroid mass m in the form

$$\log N = a_1 \log m - \log N_1 \tag{25}$$

where the constant a_1 is the slope of the curve of log N against log m and N_1 is the number of meteors with masses equal to or greater than 1 gram. Determination of the constants a_1 and log N_1 yielded

$$\log N = -1.34 \log m - 2.64 \tag{26}$$

(where N is in $km^{-2}hr^{-1}$). Equation (26) is a more useful form of the meteoroid influx representation for a space-vehicle designer. It is not so accurate a representation of the data as equation (24), since it does have implicit in it an assumed luminosity coefficient.

Whipple 1963A Rate

Equations (25) and (26) are the basic equations used by Whipple (ref. 17) in determining his proposed mass-influx rate, referred to as the "Whipple 1963A flux rate." The basic difference between this proposed influx and equation (26) as used by Hawkins and Upton is the luminosity coefficient used in calculating meteoroid masses. Since this coefficient is the basic difference, Whipple adopted equation (26) and corrected it to a new luminous efficiency in the following manner: Equation (7), with $\tau = \tau_o v$, shows the mass m as

$$m = \frac{2}{\tau_o} \int_t^{t_e} \frac{I}{v^3}\, dt \tag{7}$$

Since the masses of Hawkins and Upton (ref. 26) differ from the mass of Whipple (ref. 17) only by a different luminosity coefficient, the ratio between the two mass values is

$$\frac{m_W}{m_H} = \frac{\tau_{o,H}}{\tau_{o,W}}$$

or

$$m_W = \left(\frac{\tau_{o,H}}{\tau_{o,W}}\right) m_H \tag{27}$$

where the subscripts W and H refer to Whipple and Hawkins, respectively. Then

$$\log m_W = \log \frac{\tau_{o,H}}{\tau_{o,W}} + \log m_H \tag{28}$$

Substituting $\log m_H$ from equation (28) into equation (26) yields

$$\log N = 1.34 \log \frac{\tau_{o,H}}{\tau_{o,W}} - 1.34 \log m - 2.64 \tag{29}$$

which can be used to correct the Hawkins and Upton equation to any value of the luminosity coefficient.

Hawkins and Upton used $\tau_o = 10^{-20.91}$. Whipple (ref. 17) proposed $\tau_o = 10^{-19.42}$; equation (29) therefore becomes, for the Whipple values,

$$\log N = -1.34 \log m - 4.63 \tag{30a}$$

(where N is in $km^{-2}hr^{-1}$) or

$$\log N = -1.34 \log m - 14.18 \tag{30b}$$

(where N is in $m^{-2}sec^{-1}$). Equations (30a) and (30b) (differing only by their units), give the proposed influx rate of Whipple (ref. 17), the Whipple 1963A flux rate. The relations of equations (30) do not contain the Earth shielding factor of 1/2 that Whipple included in his proposed influx rate. The reduction in flux by a factor of 1/2 as proposed by Whipple (ref. 17) is not realistic for the general case, since obviously the effect of Earth shielding is a function of the altitude of the vehicle, and can be 1/2 only when the vehicle is at the effective meteoroid boundary of the Earth's atmosphere.

Included in the proposed influx rate of equations (30) is an average meteoroid density consistent with the assumed luminosity coefficient. This value is 0.44 gram per cubic centimeter. The influx rate of equations (30), with an average velocity of 30 kilometers per second and an average density of 0.44 gram per cubic centimeter, has become the most widely used meteor flux model to date.

Revised Rate

As discussed in three previous sections, better values of meteoroid mean density (based on a new luminosity coefficient) and meteoroid average velocity appear to be available. It seems reasonable, therefore, to propose a meteoroid flux model based on these values. In general, equation (26) can be corrected to a new value of the luminosity coefficient τ_o by using

$$\log N = -1.34 \log m - 2.64 + 1.34 \log \frac{10^{-20.91}}{\tau_o} \tag{31}$$

Verniani (ref. 10) arrived at $\tau_o = 10^{-19.72}$ and $\rho_m = 0.2$ gram per cubic centimeter as representative of cometary meteors. If this value of τ_o is accepted as the best estimate to date, equation (31) is corrected to yield

$$\log N = -1.34 \log m - 4.23 \tag{32}$$

(where N is in $km^{-2}hr^{-1}$). As shown previously, the average velocity of the observed sample (fig. 3, p. 21) is about 30 kilometers per second. The use of equation (32) with an average velocity of 30 kilometers per second and an average density of 0.2 gram per cubic centimeter would yield a consistent flux model for the observed sample.

As discussed previously, the velocity bias of observation indicates that many particles are unobserved. Since the design engineer is more interested in the actual flux distribution than in the observed distribution, equation (32) should be further corrected to account for these inferred "unobserved" particles. The mass influx rate derived by Hawkins and Upton (ref. 26) has in it a correction of observation based on the assumption that all the large mass particles are observed. The following observational bias removal assumes that all the high-velocity meteors were observed, and that regardless of mass the low-velocity meteors went largely unobserved.

The velocity-corrected distribution yielded $\bar{v}_c = 20$ kilometers per second compared with the observed distribution value of $\bar{v}_{obs}$ of 30 kilometers per second. The decrease in average velocity was attributed to the inferred increase in the number of low-velocity particles. This increase in particle number was assumed previously to be proportional to $1/v^2$ for constant particle mass. The increase in sample number, for essentially constant mass, would thus be proportional to the square of the ratio of the sample average velocities; that is,

$$\frac{N_c}{N_{obs}} = \left(\frac{\bar{v}_{obs}}{\bar{v}_c}\right)^2 \tag{33}$$

or

$$\Delta \log N = 0.352$$

Equation (32) is then modified to yield

$$\log N = -1.34 \log m - 3.88 \tag{34}$$

(where N is in $km^{-2}hr^{-1}$). Equation (34) with $\rho_m = 0.2$ gram per cubic centimeter and $\bar{v} = 20$ kilometers per second is then a consistent meteoroid flux model for a near-Earth

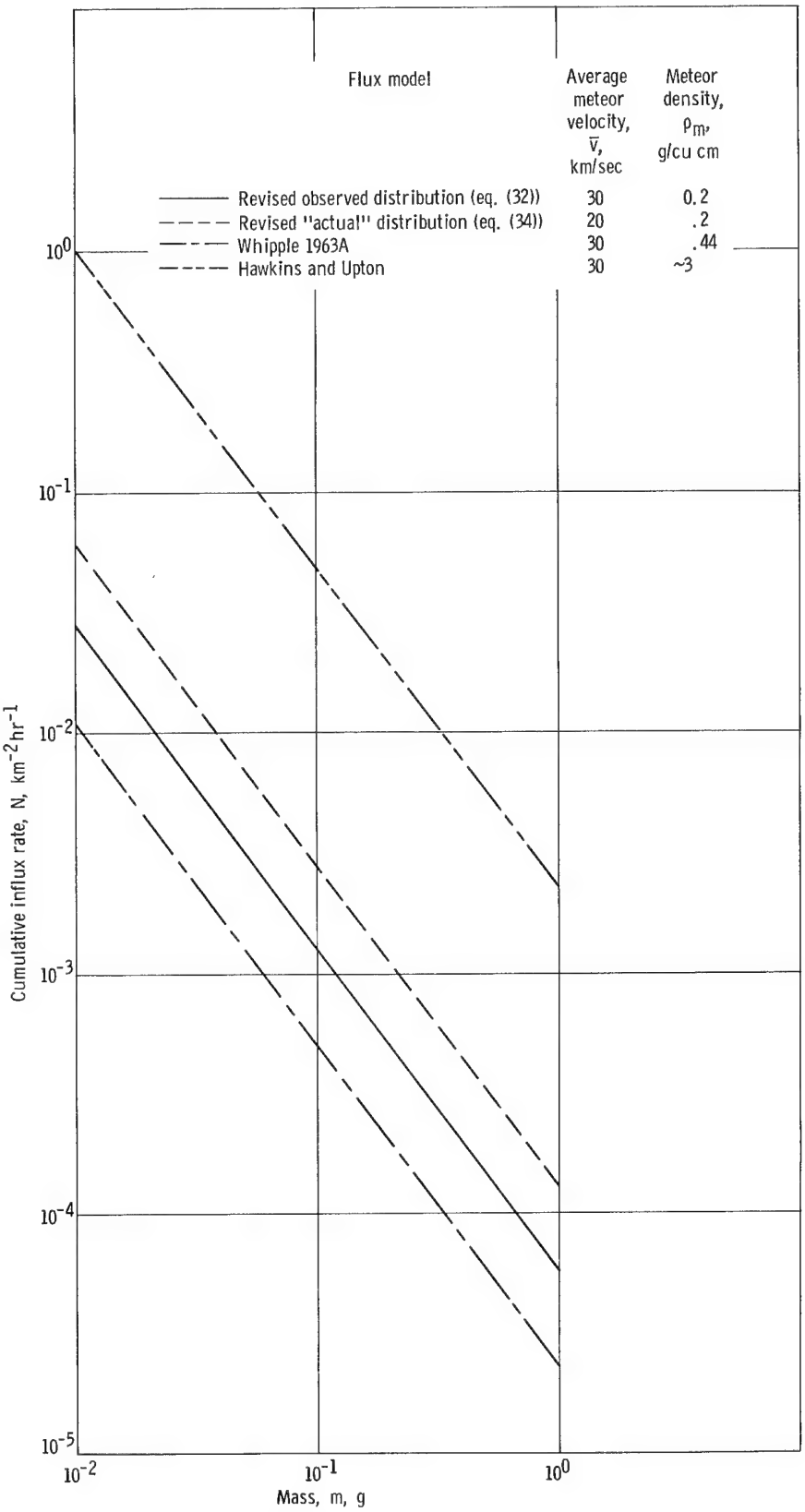

Figure 5. - Deduced influx rates based on data of Hawkins and Upton (ref. 26).

environment representing an estimate of the "actual" rather than the observed distribution. The mass range over which this model can be assumed to apply is 10^{-2} to 10^{0} gram, which is the range of the observed data.

The various flux models discussed herein along with their associated values of density and velocity are shown in figure 5. The flux models of Hawkins and Upton, Whipple 1963A, and the solid curve of equation (32) are all representative of the observed reference data, and the differences are wholly attributed to the assumed luminosity coefficient. The dashed curve is the inferred "actual" distribution as discussed previously in equation (34).

The revised actual distribution (dashed curve) indicates an increase in the meteor hazard as compared with the Whipple 1963A curve. The proposed associated lower density and velocity, however, counteract much of this increase, as shown in a later section.

EARTH SHIELDING FACTOR

When a flux model is used for meteoroid protection calculations for an Earth satellite, the influence of the Earth as a shield should be considered. Whipple recognized this influence but applied a single factor of 1/2. In reality, the Earth shielding factor E is a variable and can be so computed as a function of the altitude of the satellite above the Earth's surface that, at any altitude,

$$N_S = EN \tag{35}$$

where N is obtained from equation (31).

In calculating E, it will be assumed that the meteoroid population is isotropic. Figure 6 represents a unit hemisphere of space of unit radius, with its center at the satellite; r is the true radius of the Earth, h is the satellite altitude above the surface of the Earth, and R is the "effective" radius of the Earth. Using the effective radius of the Earth recognizes that most meteors burn out in the upper atmosphere at altitudes of 70 to 100 kilometers. The atmosphere of the Earth therefore provides an effective shield to meteoroids and thereby serves to increase the radius of the occluding body. For practical purposes, the atmosphere at 90 kilometers, or approximately 50 nautical miles, should provide an effective shield to meteoroid passage; that is, Δr = 50 miles. With the use of this assumption, the effective Earth shielding as a function of altitude can be derived from reference to the geometry of figure 6.

The shielding factor of a satellite at altitude h above the Earth's surface is determined to be

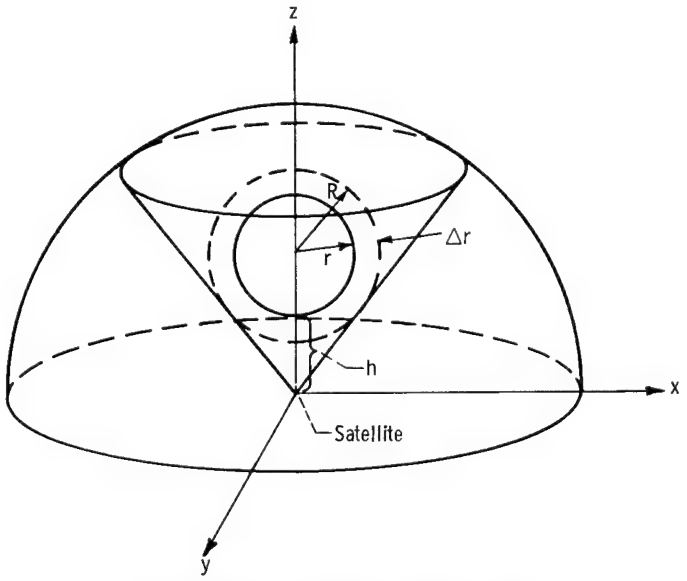

Figure 6. - Spatial geometry and definition of symbols used in calculating Earth shielding factor.

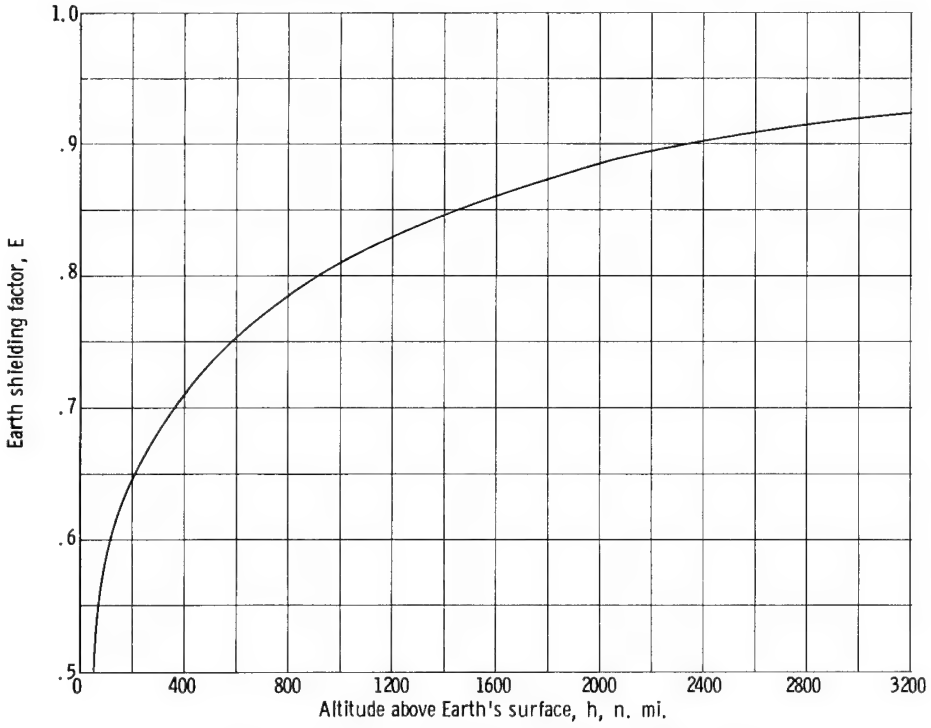

Figure 7. - Earth shielding factor as function of satellite altitude.

$$E = \frac{1}{2} + \frac{\sqrt{(r + h)^2 - (r + \Delta r)^2}}{2(r + h)} \tag{36}$$

Figure 7 shows the Earth shielding factor as a function of altitude based on the assumption that the atmosphere is an effective shield up to 50 nautical miles. The Earth's occlusion is of importance to satellites in orbit at less than about 2500 nautical miles.

DESIGN IMPLICATIONS

From the preceding discussion it is obvious that the reduction of photographic meteor data into meaningful information useful to the space-vehicle designer is not a simple and precise task. Furthermore, there are many limitations and assumptions involved in the reduction methods that can have notable effects and implications on the design protection requirements. These limitations and assumptions can best be appreciated by examining a typical relation used for predicting required armor thickness to prevent critical meteoroid damage.

Reference 1 presents an equation for required single-sheet armor thickness as a function of mission parameters and meteoroid hazard as

$$\delta = D\rho_m^{-1/3}\left(\frac{\rho_m}{\rho_t}\right)^{1/2}\left(\frac{\bar{v}}{C}\right)^{2/3}\left[\frac{\alpha A_v T}{-\ln P(0)}\right]^{1/3\beta}\left(\frac{2}{3\theta\beta + 2}\right)^{1/3\beta} \tag{37}$$

In terms of only meteoroid properties,

$$\delta = D_1\rho_m^{1/6}\bar{v}^{2/3}\left(\frac{\alpha}{\beta + 1}\right)^{1/3\beta} \tag{38}$$

where ρ_m and $\bar{v}$ are the meteor bulk density and impact velocity, respectively. The factors α and $-\beta$ are related to the meteoroid flux according to the equation

$$N = \alpha m^{-\beta} \tag{39}$$

The exponent $-\beta$ is the slope of the general curve of log N against log m (eq. (25)) and α is the same as N_1.

Meteoroid Density

In a previous section the calculation of the density for a particular meteoroid was shown to be dependent on several factors other than the data obtained from the photographic plate. In particular, the luminosity coefficient τ_0 and the drag-area coefficient ΓA, as well as the correct application of the fragmentation index, were shown to be highly influencing factors. The uncertainty introduced in the value of the meteoroid density by the uncertainty in these factors is easily seen from equation (11) as proportional to $\sqrt{\tau_0(\Gamma A)^3}$. It is impossible, however, to place uncertainty limits on either τ_0 or ΓA, since at best they are educated estimates. The treatment of large groups of data, as explained previously, is assumed to nullify the uncertainty in the drag-area coefficient and thus to reduce the uncertainty in the "average" meteoroid density primarily to a function of τ_0 (if fragmentation is assumed to be correctly applied). Fortunately, equation (38) shows that the required armor thickness for space-vehicle protection bears a very weak relation to the meteoroid density. This weak relation, which was derived for solid homogeneous particles, may be a conservative relation for the low-bulk-density, low-crushing-strength meteoroid particle.

Meteoroid Velocity

The treatment of estimated impact velocity warrants further study. The attempt herein to remove the observational bias of the data has resulted in a reduction of the average velocity of the meteor sample relative to the Earth from a nominal 30 to 20 kilometers per second. The correction presented is not precise but rather is an attempt to show an effect that can markedly influence the total meteoroid hazard. If an average meteoroid velocity relative to the Earth is to be better defined, a more precise treatment is needed in which the observational bias is removed from individual meteor cases by considering all the factors involved and the fact that all meteors are not of the same mass. The treatment presented assumed that the velocity histograms were independent of mass. It is probable that large particles will be observed regardless of their velocity; this possibility makes the correction presented invalid for this region of mass.

The value of 20 kilometers per second deduced herein as a typical or average meteoroid velocity is relative to the Earth at the limit of its upper atmosphere and is not necessarily the value that should be used in equation (38). Ideally, the value in equation (38) should be the effective meteoroid impact velocity relative to the space vehicle for its mission. Uncertainties in relative impact velocity affect the required single-sheet armor thickness drastically (proportional to $\bar{v}^{2/3}$), and a significant effort is therefore indicated for the determination of accurate values. Meteoroid relative impact velocity is a

function of the vehicle trajectory in space and the spatial meteoroid velocity distribution. The second of these two items is at present undefined. Much work remains in the definition of this spatial velocity distribution. The heliocentric as well as the geocentric relations involved are necessary, and a method of incorporation of the results into protection equations such as equation (38) must be devised for a precise analysis of the hazard. To date, meteor data are lacking for the definition of this distribution. For an Earth-orbiting vehicle at high altitude (long periods), a 20-kilometer-per-second relative impact velocity for particles in the photographic mass range may be an adequate estimate. More advanced missions, however, such as those that leave an Earth orbit or that involve orbits with short periods or high eccentricity, will require a more sophisticated analysis of the estimation of meteoroid impact velocities.

Mass-Influx Rate

The influence of the mass-influx rate on the required armor thickness in equation (38) is indicated by the values of α and β.

The value of β, the slope of the curve of log N against log m, equal to 1.34 established by Hawkins and Upton in 1958 (ref. 26) has remained unchanged. Although a more precise value of β can probably be determined from an increased sample mass range and sample number, $\beta = 1.34$ can be assumed to be sufficiently valid for use over the photographic mass range.

Uncertainties in α will reflect uncertainties in δ approximately proportional to the 1/4 power (if $\beta = 1.34$ is assumed). The value of α is seen from equation (31) to be directly related to the uncertainty in the luminosity coefficient τ_o raised to the 1.34 power. Comparing the influx rates of Whipple (eq. (30)) and Hawkins and Upton (eq. (26)) shows a two-order-of-magnitude difference in the value of α (from 2.64 to 4.63) and correspondingly in the value of flux. This variation is wholly attributable to the differences in the values used for τ_o. This indicated relation reflects the strong dependence of the required armor thickness on the absolute value of τ_o. As explained previously, this absolute value is difficult to determine; therefore, confidence in τ_o (and finally α) becomes related to the "educated guess" made in determining τ_o.

In addition to uncertainties in α (related to the accuracy of τ_o), the value of the flux will depend on the magnitude of the velocity bias of the observation and the effective removal of this bias from the observed sample. The dashed curve of figure 5 (p. 29) indicates an "actual" distribution inferred from observational data based on an approximate removal of the observational bias, as explained previously. This representation of an "actual" rather than the observed influx rate is currently felt to be more meaningful for protection calculations. A better curve could be inferred from a larger sample of data

by removal of the bias from individual meteor cases. The "probability" of observation, therefore, does not have to be made independent of mass, as explained previously.

Finally, the influx rates discussed herein should specifically be limited in use to a near-Earth environment. The effect of gravity focusing by the Earth is implicit in the measured flux rate and therefore in the inferred actual flux rate. Since the focusing effect tends to concentrate meteoroid particles in the immediate vicinity of the Earth, flux rates could be significantly different from the observed values at large distances from the Earth. The focusing effect, being velocity sensitive, requires the treatment of individual meteor cases for greater precision in the determination of the flux.

Comparison with Whipple 1963A Hazard

The meteoroid hazard as proposed herein based on the inferred "actual" flux and revised values of density and velocity can be compared with the Whipple 1963A hazard on the basis of equation (38). The ratio of the required armor thickness for the revised hazard δ_R based on the dashed-curve environment model proposed herein to the armor thickness given by the Whipple 1963A hazard model δ_W for the same mission is given by

$$\frac{\delta_R}{\delta_W} = \left(\frac{\rho_{m,R}}{\rho_{m,W}}\right)^{1/6} \left(\frac{\bar{v}_R}{\bar{v}_W}\right)^{2/3} \left(\frac{\alpha_R}{\alpha_W}\right)^{1/3\beta} \tag{40}$$

The following table lists the various input values for each model:

Model	Meteoroid density, ρ_m, g/cu cm	Average meteoroid velocity, $\bar{v}$, km/sec	Slope of mass against influx rate, β	log α
Whipple 1963A	0.44	30	1.34	-4.63
Revised environment (dashed curve, fig. 5)	.2	20	1.34	-3.88

Substituting into equation (40) the various values of ρ_m, $\bar{v}$, β, and α for each model yields

$$\frac{\delta_R}{\delta_W} = 1.03 \tag{41}$$

The revised hazard indicates that about 3 percent more armor is needed than predicted by the Whipple 1963A hazard model. This minor increase in required armor thickness is due to the counterbalancing effects of an increased indicated flux and a decreased average impact velocity. For all practical purposes the two models yield the same armor requirements.

Meteoroid Structure and Shape

Two major factors have arisen in the determination of the average meteoroid density that can have a further marked influence on the required protection. These factors relate to the shape and the structure of the meteoroids and the basis of available impact relations. Current knowledge of penetration and damage effects due to the impact of hypervelocity particles (e.g., eq. (38)) has been obtained from experimental and theoretical studies based on solid homogeneous particles, usually spherical or cylindrical (equal length and diameter) in shape, and with relatively large crushing strengths. Current estimates of the meteoroid properties, as described herein, however, indicate that meteoroid particles may be substantially different from the man-made particles in both structure and shape.

First, it is believed that meteoroids may vary considerably in shape and range possibly from long needlelike rods to flat plates. Experimentally, the shape of a solid impacting particle and its orientation at impact have been shown to have a major effect on the resulting penetration (e.g., ref. 27). If these same effects persist for meteoroids, significant variations in impact damage may result from individual meteoroid particles of the same nominal characteristics, that is, mass, density, and velocity.

Secondly, and perhaps more important, meteoroid particles, by virtue of their known constituents, low bulk density, and possible origins, are believed to possess relatively low crushing strength with a structure containing a heterogeneous distribution of mass. If this is indeed true, then the resulting impact effects could be different from the currently available solid-particle relations, and, hopefully, less severe. Furthermore, if such differences exist, it would be important to determine the possible influence on these differences of such factors as meteoroid velocity, shape, and mass. Theoretical and experimental investigations may shed some light on possible impact differences, while additional meteor astronomy techniques or spacecraft experiments may be useful for further structure and shape determinations.

CONCLUDING REMARKS

It is shown herein how photographic meteor data and methods of analysis assembled

from various scientific sources are evaluated and interpreted for use in the design and development of meteoroid protection for large spacecraft components. It was indicated, however, that considerable uncertainties remain in astronomically derived meteoroid properties. Since the pertinent meteoroid properties for the larger particles, which constitute a significant threat to space devices with large vulnerable areas, cannot be obtained by practical flight experiments, further effort should be directed toward the reduction of the uncertainties in the photographic meteor analysis process. Efforts are needed to investigate the impact characteristics of meteoroid-type particles as discussed herein and to define more accurately meteoroid structure, shape, and composition.

Lewis Research Center,
National Aeronautics and Space Administration,
Cleveland, Ohio, May 7, 1965.

APPENDIX - SYMBOLS

A	shape factor
A_v	vehicle vulnerable area
a	slope of magnitude influx rate
a_1	slope of mass influx rate
a_{obs}	observed meteor acceleration
a_t	theoretical meteor acceleration
b	ratio of minor axis of meteoroid particle to major axis
C	sonic velocity of impacted target
D	constant in penetration equation
D_1	constant
E	Earth shielding factor
h	altitude of satellite above Earth's surface
I	intensity of light given off by meteor
K	$\left[-\left(\frac{1}{\rho v^2}\frac{dv}{dt}\right)^3 \int \frac{I}{v^3}\,dt\right]^{-1/3}$
M_p	photographic magnitude
m	meteoroid mass
m_e	meteoroid mass at end of meteor
m_∞	meteoroid mass before it enters Earth's atmosphere
N	cumulative influx rate
N_c	corrected cumulative influx rate
N_{obs}	observed cumulative influx rate
N_s	Earth-shielded cumulative influx rate
N_0	cumulative influx rate of zero-magnitude meteors
N_1	cumulative influx rate of 1-gram particles (same as α)
n	exponent
P	penetration
$P(0)$	probability of no critical damage
Q	aphelion distance
R	effective radius of Earth
r	mean radius of Earth
Δr	difference between effective radius and mean radius of Earth, $R - r$
S	frontal area of meteor
s	mass loss parameter
s_o	mass loss parameter at particular point on meteor trail
T	mission time
t	time
t_e	time at end of meteor
v	meteoroid velocity
$\bar{v}$	average meteoroid velocity
$\bar{v}_c$	corrected average velocity
$\bar{v}_{obs}$	observed average velocity
α	cumulative influx rate of 1-gram particles (same as N_1)
β	slope of mass agsinst influx rate (1.34)
Γ	particle drag coefficient

δ	required armor thickness to prevent critical damage
θ	constant in penetration equation (2/3)
ρ	atmospheric density
ρ_m	meteoroid density
ρ_t	target material density
τ	luminous efficiency
τ_o	luminosity coefficient
χ	fragmentation index

Subscripts:

H	Hawkins
R	revised
W	Whipple

REFERENCES

1. Loeffler, I. J.; Lieblein, Seymour; and Clough, Nestor: Meteoroid Protection for Space Radiators. Progress in Astronautics and Aeronautics. Vol. II. Academic Press, Inc., 1963, pp. 551-579.

2. Dubin, Maurice; and McCracken, Curtis W.: Measurements of Distribution of Interplanetary Dust. Astron. J., vol. 67, no. 5, June 1962, pp. 248-256.

3. Hastings, Earl C., Jr.: The Explorer XVI Micrometeoroid Satellite - Supplement 1, Preliminary Results for the Period January 14, 1963, through March 2, 1963. NASA TM X-824, 1963.

4. Watson, F. G.: Between the Planets. Harvard Univ. Press, 1956.

5. Hawkins, Gerald S.: The Meteor Population. NASA CR-51365, 1963.

6. Whipple, F. L.: Particulate Contents of Space. Medical and Biological Aspects of the Energies of Space, P. A. Campbell, ed., Columbia Univ. Press, 1961.

7. Whipple, Fred L.; and Jacchia, Luigi G.: Reduction Methods for Photographic Meteor Trails. Smithsonian Contributions to Astrophys., vol. 1, no. 2, 1957, pp. 183-206.

8. Levin, Yuri. V.: The Physical Theory of Meteors and Meteoroid Matter in the Solar System. Pergamon Press, 1963.

9. Jacchia, L. G.: The Physical Theory of Meteors. VIII - Fragmentation as Cause of the Faint Meteor Anomaly. Astrophys. J., vol. 121, 1955, pp. 521-527.

10. Verniani, Franco: On the Luminous Efficiency of Meteors. NASA CR-55904, 1964.

11. Öpik, E. J.: Physics of Meteor Flight in the Atmosphere. Intersci. Pub., Inc., 1958.

12. Jacchia, L. G.: A Comparative Analysis of Atmospheric Densities from Meteor Decelerations Observed in Massachusetts and New Mexico. Tech. Rept. No. 10, Harvard College Observatory, 1952.

13. Whipple, F. L.: On Meteor Masses and Densities. Astron. J., vol. 57, 1956, pp. 28-29.

14. McCrosky, R. E.; and Soberman, R. K.: Results from an Artificial Iron Meteoroid at 10 km/sec. Rept. No. AFCRL X62-803, Air Force Cambridge Res. Labs., July 1962.

15. Cook, A. F.; Jacchia, L. G.; and McCrosky, R. C.: Luminous Efficiency of Iron and Stone Asteroidal Meteors. Proc. Symposium on Astronomy and Phys. of Me-

teors, 1963, pp. 209-220.

16. McCrosky, R. E.: Observations of Simulated Meteors. Smithsonian Contributions to Astrophys., vol. 5, no. 4, 1961.

17. Whipple, F. L.: On Meteoroids and Penetration. Smithsonian Astrophys. Observatory, 1963.

18. Whipple, F. L.: A Comet Model. I - The Acceleration of Comet Encke. Astrophys. J., vol. 111, Mar. 1950, pp. 375-394.

19. Öpik, E. J.: The Masses and Structures of Meteors. Meteors, T. R. Kaiser, ed., Pergamon Press, 1955.

20. Öpik, E. J.: Problems in the Physics of Meteors. Am. J. Phys., vol. 26, no. 2, Feb. 1958, pp. 70-80.

21. Verniani, F.: On the Density of Meteoroids. II. The Density of Faint Photographic Meteors. Nuovo Cimento, ser. 10, vol. 33, no. 4, Aug. 16, 1964, pp. 1173-1184.

22. Dauvillier, A.: Cosmic Dust. George Newnes, Ltd., 1963.

23. Donn, Bertram: The Origin and Nature of Solid Particles in Space. Ann. N.Y. Acad. Sci., vol. 119, Nov. 11, 1964, pp. 5-16.

24. Hawkins, G. S.; and Southworth, R. B.: The Statistics of Meteors in the Earth's Atmosphere. Smithsonian Contributions to Astrophys., vol. 2, no. 11, 1958, pp. 349-364.

25. McCrosky, R. E.; and Posen, A.: Orbital Elements of Photographic Meteors. Smithsonian Contributions to Astrophys., vol. 4, no. 2, 1961, pp. 15-84.

26. Hawkins, G. S.; and Upton, E. K. L.: The Influx Rate of Meteors in Earth's Atmosphere. Astrophys. J., vol. 128, no. 3, Nov. 1958, pp. 727-735.

27. Charters, A. C.: A Critique of Accelerator Techniques for Hypervelocity Impact. Proc. Sixth Symposium on Hypervelocity Impact (DDC No. AD 423798), vol. 1, Aug. 1963, pp. 1-40.

"The aeronautical and space activities of the United States shall be conducted so as to contribute . . . to the expansion of human knowledge of phenomena in the atmosphere and space. The Administration shall provide for the widest practicable and appropriate dissemination of information concerning its activities and the results thereof."

—NATIONAL AERONAUTICS AND SPACE ACT OF 1958

NASA SCIENTIFIC AND TECHNICAL PUBLICATIONS

TECHNICAL REPORTS: Scientific and technical information considered important, complete, and a lasting contribution to existing knowledge.

TECHNICAL NOTES: Information less broad in scope but nevertheless of importance as a contribution to existing knowledge.

TECHNICAL MEMORANDUMS: Information receiving limited distribution because of preliminary data, security classification, or other reasons.

CONTRACTOR REPORTS: Technical information generated in connection with a NASA contract or grant and released under NASA auspices.

TECHNICAL TRANSLATIONS: Information published in a foreign language considered to merit NASA distribution in English.

TECHNICAL REPRINTS: Information derived from NASA activities and initially published in the form of journal articles.

SPECIAL PUBLICATIONS: Information derived from or of value to NASA activities but not necessarily reporting the results of individual NASA-programmed scientific efforts. Publications include conference proceedings, monographs, data compilations, handbooks, sourcebooks, and special bibliographies.

Details on the availability of these publications may be obtained from:

SCIENTIFIC AND TECHNICAL INFORMATION DIVISION

NATIONAL AERONAUTICS AND SPACE ADMINISTRATION

Washington, D.C. 20546